nature COMMUNICATIONS

ARTICLE

Received 28 May 2014 | Accepted 16 Oct 2014 | Published 21 Nov 2014

DOI: 10.1038/ncomms6575

Larval dispersal drives trophic structure across Pacific coral reefs

Adrian C. Stier[1,2,3,*], Andrew M. Hein[3,4,*], Valeriano Parravicini[5,6,7] & Michel Kulbicki[6]

Top predators are a critical part of healthy ecosystems. Yet, these species are often absent from spatially isolated habitats leading to the pervasive view that fragmented ecological communities collapse from the top down. Here we study reef fish from coral reef communities across the Pacific Ocean. Our analysis shows that species richness of reef fish top predators is relatively stable across habitats that vary widely in spatial isolation and total species richness. In contrast, species richness of prey reef fish declines rapidly with increasing isolation. By consequence, species-poor communities from isolated islands have three times as many predator species per prey species as near-shore communities. We develop and test a colonization–extinction model to reveal how larval dispersal patterns shape this ocean-scale gradient in trophic structure.

[1] National Center for Ecological Analysis and Synthesis, 735 State Street, Santa Barbara, California 93101, USA. [2] Department of Zoology, University of British Columbia, #4200-6270 University Boulevard, Vancouver, British Columbia, Canada V6T 1Z4. [3] Department of Biology, University of Florida, Gainesville, Florida 32611-8525, USA. [4] Department of Ecology and Evolutionary Biology, Princeton University, Princeton, New Jersey 08544-2016, USA. [5] CRIOBE, USR 3278 CNRS-EPHE-UPVD, LABEX Corail, University of Perpignan, Perpignan 66860, France. [6] Institut de Recherche Pour le Développement, UR 227 Laboratoire Arago, Banyuls BP 44—66651, France. [7] CESAB-FRB, Immeuble Henri Poincaré, Domaine du Petit Arbois, Aix-en-Provence 13857, France. * These authors contributed equally to this work. Correspondence and requests for materials should be addressed to A.C.S. (email: Adrian.Stier@gmail.com) or to A.M.H. (email: ahein@princeton.edu).

Top predators are often conspicuously absent from isolated habitats[1–8]. Explanations for such spatial variation in trophic structure are numerous: predators often have greater resource requirements[9–11], larger body sizes[12], smaller population sizes[13] and slower population growth rates[14] than species lower in the food web. Moreover, in some ecosystems, predators are poorer dispersers than their prey, making it less likely that they will colonize isolated habitats, let alone persist there[1,15]. In marine systems, however, genetic estimates of dispersal distances provide some evidence that species higher in the food web disperse more widely than species in lower trophic levels[16]. If predators disperse widely, serial influx of colonists could rescue isolated predator populations from extinction. An immediate question, then, is how do differences in the dispersal patterns of predators and their prey affect geographic patterns of community trophic structure?

To answer this question, we analysed a database of published species lists from 35 major coral reef fish communities across the Pacific Ocean consisting of 1,350 total species. Using diet and life history information, we classified each species as either a piscivorous top predator (hereafter predator) or as a species lower on the food chain (hereafter prey). The ratio of the number of predator species to the number of prey species (predator–prey ratio[17], R; Fig. 1, circle colour) and total reef fish species richness (circle size) vary widely among Pacific coral reef communities. Total reef fish species richness decreases with increasing isolation as in other systems[18,19] and predator–prey ratio varies among islands by a factor of 3 (range: 0.34–1.1 predator species per prey species; Fig. 1). However, in stark contrast to patterns reported from other ecosystems[20], the coral reef communities with the highest predator–prey ratios are species-poor communities from the most isolated habitats (for example, Midway, Tuvalu; Fig. 1 inset), whereas communities located near large landmasses (for example, Palau, Vanuatu) have high total species richness and low predator–prey ratios.

Two features of Pacific coral reef communities are at odds with theory and observations from other systems. First, predator–prey ratio is high in isolated communities and low in proximate ones. Second, predator–prey ratio is negatively correlated with total reef fish species richness (Fig. 1, inset) instead of being positively correlated with, or invariant of total richness as in many terrestrial and aquatic ecosystems[20]. These findings contradict theoretical predictions[13,21] and empirical studies of other ecosystems, which suggest that species highest in the food web should be most sensitive to habitat isolation[4,10,12,22]. Here we develop a mathematical dispersal–colonization–extinction framework that resolves both of these discrepancies. The framework models species composition in a given habitat as an equilibrium between colonization of new species and extinction of those already present[23], but builds on this concept by incorporating a basic life history trait of reef fish, the duration of pelagic (open ocean) larval dispersal, which can influence species' dispersal distances[24]. We model larval dispersal to predict colonization rate at focal reefs, and use colonization rate to predict how species richness and predator–prey ratio vary across space.

Results

Modelling framework. Most reef fishes exhibit a multi-stage lifecycle involving a dispersive larval stage, followed by a non-dispersive adult stage. The length of time larvae spend in the dispersive stage is known as pelagic larval duration (PLD). Limited dispersal due to limited PLD has been proposed to explain why total reef fish species richness is lower in more isolated habitats and why species that do occur in isolated habitats have higher mean PLD than those inhabiting near-shore habitats[18,25]. In general, short-term estimates of dispersal distance are positively correlated with PLD among marine species, although the strength of this relationship varies across the range of PLDs[26]. In this study, we are most interested in dispersal that allows species to colonize new habitats over long ecological timescales (that is, hundreds to thousands of fish generations). Genetic estimates of dispersal distances may provide the best available indices of dispersal distance on such timescales. Genetic estimates of dispersal distance are strongly correlated with PLD, and also agree reasonably well with dispersal distance estimates from computational Lagrangian particle models, which assume that marine larvae disperse like passive particles through the plankton[24]. Here we take an analytical approach that includes PLD along with other basic features of the larval dispersal process.

To relate PLD to dispersal and colonization rates of predators and prey, we use a diffusion–advection–mortality model[27], which describes dispersal of fish larvae from large source populations (Figs 2,3; full model described in Supplementary Methods). The ratio of predator colonization rate (C_{pred}) to prey colonization rate (C_{prey}) at a given location obeys

$$\frac{C_{\mathrm{pred}}}{C_{\mathrm{prey}}} \propto e^{\left[\frac{(\tau_{\mathrm{pred}}-\tau_{\mathrm{prey}})d^2}{4\sigma\tau_{\mathrm{pred}}\tau_{\mathrm{prey}}}\right]}, \qquad (1)$$

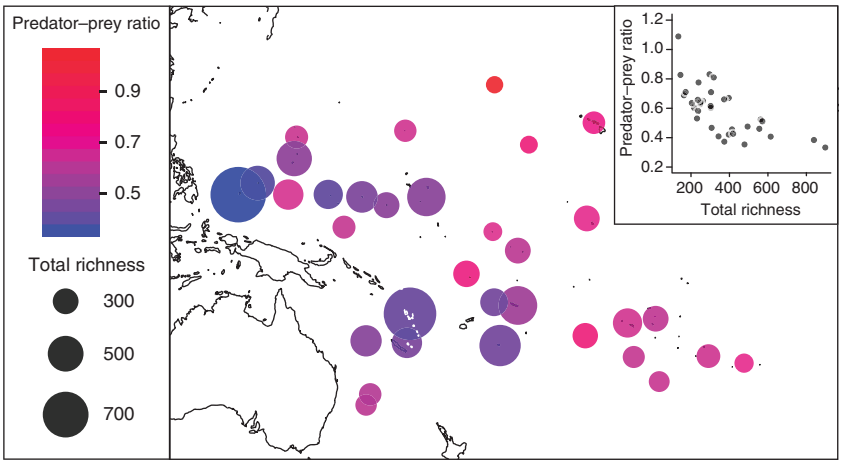

Figure 1 | Predator–prey ratio and total species richness in coral reef fish communities from 35 Pacific habitats. Circle size increases with increasing total species richness (# of predator species + # of prey species); colour indicates low (blue) or high (red) predator–prey ratio. Inset showing that predator–prey ratio decreases strongly with increasing total species richness.

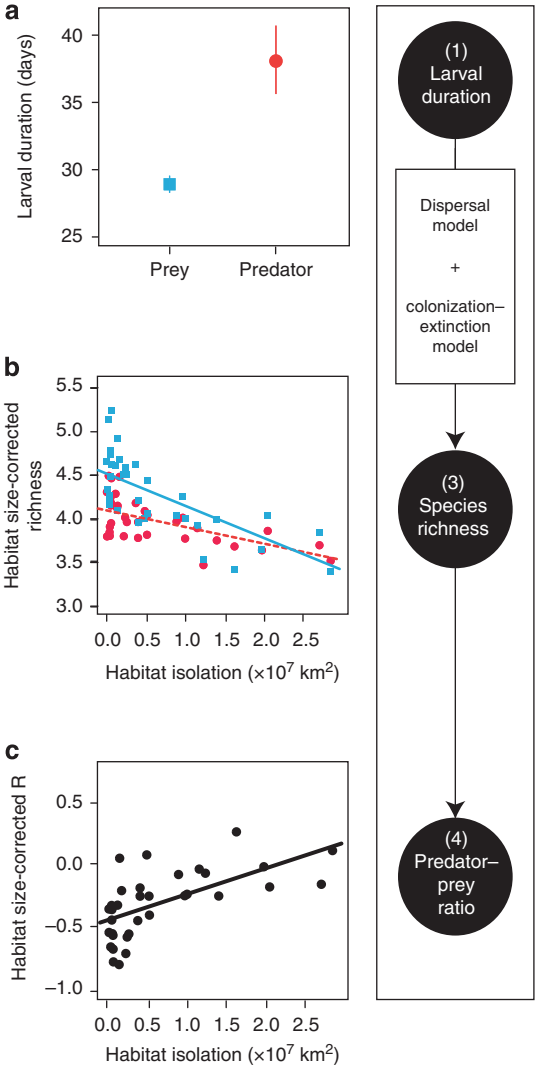

Figure 2 | Integration of dispersal model with colonization–extinction model and fitting of model to Pacific reef fish data. (**a**) Larval duration data indicate that predators (red) have longer mean PLD than prey (blue; $\tau_{prey} = (28.3, 29.5)$ days, $\tau_{pred} = 38.1$ (35.6, 40.7) days, mean number of days (lower, upper s.e.m.); *t*-test: $t = 3.92$, $P < 0.001$, n prey = 347, n predators = 35, means and s.e. back-transformed from log scale). (**b**) Model predicts that predators' longer larval durations ($\tau_{pred} > \tau_{prey}$) will cause a relatively shallow decay of predator richness (red) compared with relatively rapid decay of prey richness (blue) with increasing habitat isolation. (**c**) Mechanistic model of predator-prey ratio fitted to data. Model predicts that the predator-prey ratio (R) increases with habitat isolation, measured as squared distance from the focal site to the nearest landmass with area $>10^4\,km^2$ (see Methods for statistics). Predictions are robust to other metrics of isolation.

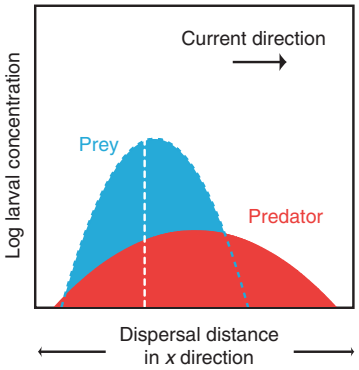

Figure 3 | Diagram illustrating differential spreading of predator larvae. Larval concentration of a species of predator (red) and prey (blue) at different distances from a source population (dashed vertical white line), given that predator spends more time dispersing than prey. Larval dispersal is modelled using a diffusion-advection-mortality model. Larvae originate at a source location and larval concentration, l_i of prey ($i = 1$) or predators ($i = 2$) is governed by the equation, $\frac{\partial l_i}{\partial t} = \sigma \Delta l_i - u\frac{\partial l_i}{\partial x} - v\frac{\partial l_i}{\partial y} - \mu_i l_i$, in two dimension (2D; Δ is 2D Laplacian, u and v are mean speeds of advective currents in x and y directions, respectively, σ represents the effective diffusivity of larvae and μ_i is mortality rate)[27].

where τ_{pred} is predator PLD, τ_{prey} is prey PLD, d is the distance between the source of larvae and the focal habitat and σ ($\sigma > 0$) is the effective diffusivity of predator and prey larvae during dispersal. The ratio of predator larvae to prey larvae colonizing a site will increase with increasing habitat isolation if predators spend more time drifting in the plankton than their prey (that is, $\tau_{pred} > \tau_{prey}$). This is because a longer PLD causes predator larvae to spread farther from their point of release (Fig. 3), creating a distribution of predator larvae that is spread more uniformly over space than the distribution of prey larvae (Supplementary Methods section 4.1 and Supplementary Fig. 2 discuss multiple larval sources). Data from 382 species of Indo–Pacific reef-associated fish from a recently published database[28] (Supplementary Data 1; n prey = 347, n predators = 35) indicate that mean predator PLD is 28% longer than mean prey PLD (Fig. 2a). Equation (1) therefore predicts that the ratio of predator to prey colonization rates should increase with increasing habitat isolation.

To connect colonization rates with standing species richness and predator–prey ratio, we use a colonization–extinction model[23] (Fig. 2b,c). In keeping with classical models[13], we assume that species within each trophic level colonize and go extinct from habitats identically and independently. We calculate the predator–prey ratio R in a focal habitat as the ratio of the equilibrium number of predator species (S_{pred}) to the equilibrium number of prey species (S_{prey}), $R = \frac{S_{pred}}{S_{prey}} \propto \frac{p^*_{pred}}{p^*_{prey}}$, where p^*_{pred} and p^*_{prey} are the equilibrium probabilities that any given predator or prey species occur in the community (Supplementary Methods). The dynamics of p_{pred} and p_{prey} can be modelled by the differential equations, $\frac{dp_{prey}}{dt} = C_{prey}(1 - p_{prey}) - E_{prey}p_{prey}$ and $\frac{dp_{pred}}{dt} = C_{pred}(1 - p_{pred}) - E_{pred}p_{pred}$, with equilibrium $p^*_i = 1/(1 + \frac{E_i}{C_i})$, where the subscript i denotes predators or prey and C_i and E_i denote colonization and extinction rates, respectively[13] (we discuss coupling between predators and prey in Supplementary Methods). When the equilibrium occurrence probability of any given species is small,

$$R \propto \left(\frac{C_{pred}}{C_{prey}}\right)\frac{E_{prey}}{E_{pred}}. \quad (2)$$

Predator–prey ratio is proportional to the ratio of predator to prey colonization rates, which may vary with habitat isolation, and proportional to the ratio of extinction rates, which will not generally depend directly on habitat isolation.

Combining the model of larval dispersal described above (equation (1)) with the equilibrium model for predator–prey ratio (equation (2)) shows how predator–prey ratio depends on habitat

isolation:

$$R = r_0\left(\frac{C_{\text{pred}}}{C_{\text{prey}}}\right) = r_1 e^{\left[\frac{\left(\tau_{\text{pred}} - \tau_{\text{prey}}\right)d^2}{4\sigma\tau_{\text{pred}}\tau_{\text{prey}}}\right]}, \qquad (3)$$

where r_0 and r_1 are positive constants that capture factors that do not depend on isolation (for example, differential larval production, differential extinction rates and larval mortality rates). Equation (3) states that predator–prey ratio should increase with increasing isolation distance when predator PLD is longer than prey PLD (that is, $\tau_{\text{pred}} > \tau_{\text{prey}}$). It also predicts the form of the function relating isolation distance, d, to predator–prey ratio, R. Below we describe how this predicted functional form can be fit to data, and explore whether the model developed above can account for patterns evident in the Pacific reef fish data.

Fitting models to data. By log (ln) transforming both sides of equation (3), we can fit the predicted function of $\ln(R)$ as a linear function of d^2 directly to the predator–prey ratio data shown in Fig. 1 (fit shown in Fig. 2c, statistical models and spatial autocorrelation discussed in Methods). In what follows, we will refer to d^2 as 'habitat isolation' and d as 'isolation distance'. Figure 2c shows that predator–prey ratio increases with increasing habitat isolation as predicted by our model ($P = 1.8 \times 10^{-4}$; habitat isolation measured as squared distance to nearest landmass with area $> 10^4\,\text{km}^2$; other isolation metrics yield similar results; Supplementary Methods). This occurs because predator richness (Fig. 2b, red circles, dashed line) is less sensitive to habitat isolation than is prey richness (Fig. 2b, blue squares, solid line, $P = 9.5 \times 10^{-6}$, $r^2 = 0.78$) as our model predicts, given that predators have longer PLDs than prey (Fig. 2a). The model thus resolves the first discrepancy between observations from other ecosystems and our observations from coral reef communities, that isolated reef communities have the highest predator–prey ratios. Isolated communities have high predator–prey ratios because at their times of settlement, predator larvae are spread more uniformly across space than prey larvae. This makes predator larval supply (Fig. 3), colonization rate and, consequently, species richness (Fig. 2b) relatively insensitive to habitat isolation. Prey richness falls more rapidly with increasing habitat isolation causing predator–prey ratio to rise as isolation increases (Fig. 2c).

A second prediction follows from the form of the functions relating S_{pred} and S_{prey} to habitat isolation. When currents spread larvae but directional advection is weak, our model predicts that the richness of species in trophic group i is $S_i \approx K_i \exp[\frac{-d^2}{4\sigma\tau_i}]$, where K_i is a trophic level-specific constant (Supplementary Methods). Substituting this expression for prey richness into the corresponding expression for predator richness reveals that $S_{\text{pred}} \propto S_{\text{prey}}^{\lambda}$; predator richness should be a power function of prey richness with exponent $\lambda = \tau_{\text{prey}}/\tau_{\text{pred}}$. Figure 4 shows this predicted function fitted to the Pacific reef fish data. Communities with higher total richness (that is, points closer to the upper right corner of Fig. 4) are farther from the dashed one-to-one line. As predicted, the relationship between S_{pred} and S_{prey} is described well by a power function (exponent = 0.59, 95% confidence interval (CI) = (0.5, 0.68), $P = 4.9 \times 10^{-16}$, $r^2 = 0.89$); a power function provides better prediction of the data than the linear function that would result if predator–prey ratio were constant (Akaike's Information Criterion (AIC) power model: 313; AIC linear model: 317), which is consistent with the observation that predator–prey ratio declines as total species richness increases (Fig. 1, inset). Because the power function exponent λ is determined solely by predator and prey PLDs, we can independently estimate λ from the PLD data shown in Fig. 2a. Dividing mean prey PLD by mean predator PLD indicates that $\lambda = 0.77$ (delta method 95% CI = (0.65, 0.88)), close to the fitted value of 0.59 (0.5, 0.68), particularly considering that the former ignores effects of prevailing directional currents on dispersal patterns. Critically, both predicted and observed exponents are less than 1. The model correctly predicts that communities with low overall richness will have the highest predator–prey ratios, resolving the second discrepancy between patterns of predator–prey ratio in other ecosystems and patterns in Pacific coral reef communities.

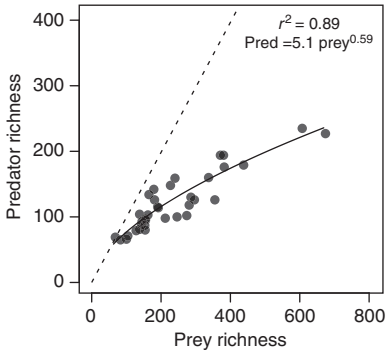

Figure 4 | Relationship between reef fish prey and predator species richness in Pacific coral reef communities. Functional form (power function) predicted from dispersal–colonization–extinction framework and fitted using generalized nonlinear least squares accounting for spatial autocorrelation. Data from 35 islands across the Pacific (1,350 total species).

Discussion

The qualitative predictions of our model are robust to changes in our assumptions about reef fish dispersal and colonization. For example, the simplified model of colonization–extinction dynamics of equation (2) does not account for the dependence of predators on the presence of their prey[9–11]. Incorporating this prey dependence (Supplementary Methods) shows that the predator–prey ratio R can still increase with habitat isolation in a manner consistent with equation (3) for a range of habitat isolation values. The coupled predator–prey colonization–extinction model developed in Supplementary Methods reveals that predator diet specialization also affects the relationship between predator–prey ratio and habitat isolation. If predators are highly specialized, predator–prey ratio will initially increase as habitat isolation increases, but will quickly begin to decline as the prey of specialist predators disappear from isolated habitats, and predators are thereby driven extinct. However, when predators are generalists as in the case of many reef fish predators[29], R will continue to increase with habitat isolation over a wide range of isolation values as observed in the Pacific reef fish data. Intuitively, this is because generalist predators can persist on a wide range of different prey and the absence or loss of prey from isolated habitats only affects a predator if all of that predator's prey species are simultaneously absent. The coupling between predator and prey richness will be even weaker if predators can persist by eating juvenile conspecifics and juveniles of other piscivorous species[29]. In the extreme case where predators eat juveniles of all species, the coupling between predator and prey equations becomes very weak and the uncoupled equations presented above are approximately recovered (Supplementary Methods).

Processes other than those described by our model undoubtedly contribute to the variation present in Figs 1, 2b,c and 4. We do not consider effects of predators on prey extinction[30–32], effects of complex trophic structure[10], local speciation[33], other life

history characteristics such as body size, diurnal or nocturnal activity and schooling behaviour[28], nor do we consider complex ocean currents[34]. The amount of population self-recruitment, post-arrival establishment success and species body sizes may differ among predators and prey[28], leading to differences in predator and prey extinction rates (equation (2)). However, these differences will not affect the isolation dependence of predator–prey ratio (that is, they affect r_1 only in equation (3)) unless they generate a correlation between extinction rate and habitat isolation. Because we are interested in the isolation dependence of the predator–prey ratio, we do not consider these factors explicitly. Previous studies have noted that selective overharvesting of top predators may compound effects of habitat loss on predator richness[8]. In marine ecosystems, disproportionate fishing pressure on top predators (that is, 'fishing down food webs') is well documented[35–37], although local anthropogenic extinctions are seldom described in reef fish systems. In Supplementary Methods, we explore whether fishing pressure on top predators alone can account for the patterns of reef fish predator–prey ratio described above. Statistical models that contain indices of fishing pressure but lack the functional relationship between predator–prey ratio and habitat isolation derived above provide a poor fit to data. Overfishing of top predators alone does not account for the patterns reported here.

Mounting evidence suggests that species' dispersal patterns shape community and food web structure in many ecosystems[38–42]. For example, competing reef fish species in the Great Barrier Reef ecosystem appear to have different dispersal abilities, and this difference may explain the complex patterns of species coexistence observed across the Great Barrier Reef[40]. Dispersal has also been implicated as a potential cause of geographic variation in the structure of species interactions within local communities (for example, seed dispersal networks on insular versus mainland habitats[41]). On shorter timescales, it is possible to show experimentally that differences in colonization rates among local habitats cause differences in community structure across a landscape[38]. For example, invertebrate predators and prey colonize experimental pond habitats at different rates. This differential colonization generates a spatial gradient in the relative abundances of species occupying different positions in a food web[38]. Variation in colonization rates across a landscape can also create spatial variation in functional structures within local food webs and the rate at which these structures develop during community assembly[39,43]. The results presented here suggest that effects of dispersal on community trophic structure can extend over a very large spatial scale.

Our study reveals that marine predator species richness is less sensitive than prey richness to habitat isolation, and that this asymmetry causes major variation in trophic structure across Pacific coral reefs. The modelling framework developed here moves from individuals to ecosystems, illustrating how attributes of individual predator and prey larvae influence the dispersal of larval populations, and ultimately create standing variation in predator and prey species richness at an oceanic scale. These results add to a growing body of evidence suggesting that careful consideration of organismal movement may help explain the structure of the ecological communities in ecosystems across the globe. Given the suite of anthropogenic threats facing reef ecosystems[44] and top predators more generally[45], a renewed focus on the mechanisms that govern community structure is essential.

Methods

Habitat isolation and coastal length. For each of the 35 focal sites, we measured the great circle distance from the centroid of the site to the nearest large potential source of larvae, defined as any landmass $>10^4$ km^2 (landmass size computed using a global equal area Behrmann projection) that contained coral reef habitat (alternative isolation metrics are discussed in Supplementary Methods). We used coastal length as a measure of habitat size for each focal habitat. Coastal length was computed as the total length of the coastline of each island or set of islands at each of the 35 sites in our database. Lengths of coastlines were measured using SRTM30 PLUS bathymetry (Shuttle Radar Topography Mission) available at http://topex.-ucsd.edu/WWW html/srtm30 plus.html.

Species lists and assignment of trophic position. Our data set included species lists from 35 islands/archipelagos with coral reef habitat and included 1,350 shallow-water reef fish species compiled in a recently published reef fish species incidence database[46]. Seventy-five percent of fish species fell into 23 families that are readily detected during surveys: Gobiidae, Labridae, Pomacentridae, Apogonidae, Serranidae, Muraenidae, Chaetodontidae, Scorpaenidae, Syngnathidae, Ophichthidae, Tripterygiidae, Callionymidae, Carangidae, Pseudochromidae, Lutjanidae, Bothidae, Pomacanthidae, Engraulidae, Soleidae, Pterelectridae, Monacanthidae, Clupeidae and Lethrinidae. We restricted our analyses to these common families. Including species from all families did not qualitatively change our results. We defined the adult trophic position (that is, predator or prey) of each species using diet, morphology and behaviour information from fishbase (http://www.fishbase.org) and the primary literature, acknowledging that predation risk in coral reef fishes is high during the early life stage for nearly all species regardless of their trophic position as adults[29]. Predators were defined as species that consumed fish as $\geq$50% of their diets as adults. We scored each potential prey species with a palatability score. Palatability 1 is preferred prey (that is, prey that are most heavily targeted by predators); palatability 2 is occasional prey (that is, prey that are not specifically targeted by predators but are eaten occasionally); palatability 3 is rare prey that are seldom targeted by predators; and palatability 4 is non-targeted species that are avoided by predators due to anti-predator traits such as toxins, spines, morphology or behaviour. For the purposes of our analyses, prey were defined as species smaller than 20 cm in total length with palatability scores of 1 or 2. We used this designation because many marine predators are gape limited and avoid consuming heavily armed and otherwise unpalatable species[29,47]. We also excluded mesopredators that were categorized as both prey and predators. In Supplementary Methods, we explore the sensitivity of our results to the choice of prey designation criteria (that is, palatability and size cut-offs). Our results do not change if alternative criteria are used to define which species are considered prey.

Statistical analysis. As described above, we fitted functions predicted by our theoretical framework to the Pacific reef fish data. For each predicted relationship, we accounted for spatial autocorrelation by using generalized least squares to fit a set of models with different spatial autocorrelation functions. Since we had no *a priori* expectation about the form of the spatial autocorrelation among sites, we used AIC to compare four commonly used models of spatial autocorrelation: spherical, exponential, Gaussian and rational quadratic. For each analysis, we report statistics from the fit that included the spatial autocorrelation function yielding the lowest AIC value. The linearized model of predator–prey ratio (R) had the form: $\ln(R)=\alpha_1+\alpha_2 d^2+\alpha_3\ln(\text{coastal length})+\Omega$, where α_j are regression coefficients and Ω includes spatial autocorrelation and normally distributed errors (data and model plotted in Fig. 2c). We included coastal length (a metric of habitat size) as a predictor because habitat size is known to affect species richness, and coastal length varied among the habitats included in our analysis. The Gaussian spatial autocorrelation model had the lowest AIC (AIC$=-2.5$, $r^2=0.44$). The analysis revealed a significant positive effect of isolation ($P=1.8\times10^{-4}$) on log (ln) predator–prey ratio and a significant negative effect of ln coastal length on ln predator–prey ratio ($P=4.2\times10^{-2}$).

The linearized model of predator and prey species richness had the same form as the model of predator–prey ratio, but included interactions between predictors and trophic level to allow for the possibility that predator and prey richness were affected differently by isolation and habitat size (Fig. 2b). The linearized model had the form $\ln(S)=\alpha_1+\alpha_2 d^2+\alpha_3\ln(\text{coastal length})+\alpha_4[i]+\alpha_5[i\times d^2]+\alpha_6[i\times\ln(\text{coastal length})]+\Omega$, where α_j are regression coefficients and i is an indicator variable denoting whether each datum was a predator or prey. The statistical fit with Gaussian spatial autocorrelation had the lowest AIC (AIC$=5.2$, $r^2=0.78$). There was a significant negative effect of isolation on ln richness ($P=1.6\times10^{-4}$) and an interaction between trophic level and isolation, such that the ln prey richness-isolation relationship declined more steeply with increasing isolation than the ln predator richness-isolation relationship ($P=9.5\times10^{-6}$; Fig. 2b). The effect of ln coastal length on ln richness was also significant ($P=7.4\times10^{-8}$), as was the ln coastal length $\times$ trophic level interaction ($P=3.3\times10^{-2}$), which indicated that ln prey richness increased more rapidly with increasing coastal length than did ln predator richness.

To display data on bivariate plots, we defined habitat size-corrected $R=\ln(R)-\alpha_3\ln(\text{coastal length})$, where α_3 is the fitted coastal length dependence of $\ln(R)$. For the species richness analysis, we defined habitat size-corrected predator richness $=\ln(S_{\text{pred}})-\alpha_3\ln(\text{coastal length})$, where α_3 is the fitted coastal length dependence for predators, and we defined habitat size-corrected prey richness $=\ln(S_{\text{prey}})-(\alpha_3+\alpha_6)\ln(\text{coastal length})$, where $(\alpha_3+\alpha_6)$ is the fitted coastal length dependence for prey. All analyses were conducted using the nlme package[48] in the R statistical programing language[49].

To determine the relationship between the number of predator and prey species at a given site, we modelled the predator richness as a function of prey richness using generalized nonlinear least squares to account for spatial autocorrelation among sites. As predicted, a power function relationship of the form, $y = ax^b$ provided a good fit to data (Fig. 4). Spatial autocorrelation was best described by a spherical spatial autocorrelation model (AIC = 313.3). The power function relationship between prey and predator richness accounted for most of the variation in predator richness ($r^2 = 0.89$, $P = 4.9 \times 10^{-16}$).

References

1. Kruess, A. & Tscharntke, T. Habitat fragmentation, species loss, and biological control. *Science* **264,** 1581–1584 (1994).
2. Chase, J. M. & Shulman, R. S. Wetland isolation facilitates larval mosquito density through the reduction of predators. *Ecol. Entomol.* **34,** 741–747 (2009).
3. Didham, R. K., Hammond, P. M., Lawton, J. H., Eggleton, P. & Stork, N. E. Beetle species responses to tropical forest fragmentation. *Ecol. Monogr.* **68,** 295–323 (1998).
4. Chase, J. M., Bergett, A. A. & Biro, E. G. Habitat isolation moderates the strength of top-down control in experimental pond food webs. *Ecology* **91,** 637–643 (2010).
5. Laurance, W. F. *et al.* Ecosystem decay of Amazonian forest fragments: a 22-year investigation. *Conserv. Biol.* **16,** 605–618 (2002).
6. Terborgh, J. *et al.* Ecological meltdown in predator-free forest fragments. *Science* **294,** 1923–1926 (2001).
7. Schoener, T. W. Food webs from the small to the large: the Robert H MacArthur lecture. *Ecology* **70,** 1559–1589 (1989).
8. Duffy, J. E. Biodiversity loss, trophic skew, and ecosystem functioning. *Ecol. Lett.* **6,** 680–687 (2003).
9. Holt, R. D., Lawton, J. H., Polis, G. A. & Martinez, N. D. Trophic rank and the species-area relationship. *Ecology* **80,** 1495–1504 (1999).
10. Gravel, D., Massol, F., Canard, E., Mouillot, D. & Mouquet, N. Trophic theory of island biogeography. *Ecol. Lett.* **14,** 1010–1016 (2011).
11. Lafferty, K. & Dunne, J. Stochastic ecological network occupancy (SENO) models: a new tool for modeling ecological networks across spatial scales. *Theor. Ecol.* **3,** 123–135 (2010).
12. Srivastava, D. S., Trzcinski, M. K., Richardson, B. A. & Gilbert, B. Why are predators more sensitive to habitat size than their prey? Insights from bromeliad insect food webs. *Am. Nat.* **172,** 761–771 (2008).
13. Holt, R. D. in *The Theory of Island Biogeography Revisited* (eds Losos, J. B. & Ricklefs, R. E.) (Princeton Univ. Press, 2010).
14. Wilbur, H. M., Tinkle, D. W. & Collins, J. P. Environmental certainty, trophic level, and resource availability in life history evolution. *Am. Nat.* **108,** 805–817 (1974).
15. Lomolino, M. V. Immigrant selection, predation, and the distributions of Microtus pennsylvanicus and Blarina brevicauda on islands. *Am. Nat.* **123,** 468–483 (1984).
16. Kinlan, B. P. & Gaines, S. D. Propagule dispersal in marine and terrestrial environments: a community perspective. *Ecology* **84,** 2007–2020 (2003).
17. Cohen, J. E. Ratio of prey to predators in community food webs. *Nature* **270,** 165–166 (1977).
18. Mora, C., Chittaro, P. M., Sale, P. F., Kritzer, J. P. & Ludsin, S. A. Patterns and processes in reef fish diversity. *Nature* **421,** 933–936 (2003).
19. Bellwood, D. R., Hughes, T. P., Connolly, S. R. & Tanner, J. Environmental and geometric constraints on Indo-Pacific coral reef biodiversity. *Ecol. Lett.* **8,** 643–651 (2005).
20. Warren, P. H. & Gaston, K. J. Predator-prey ratios—a special case of a general pattern. *Phil. Trans. R. Soc. Lond. B Biol. Sci.* **338,** 113–130 (1992).
21. Nachman, G. Systems analysis of acarine predator-prey interactions. II. The role of spatial processes in system stability. *J. Anim. Ecol.* **56,** 267–281 (1987).
22. Holyoak, M. & Sharon, P. L. The role of dispersal in predator--prey metapopulation dynamics. *J. Anim. Ecol.* **65,** 640–652 (1996).
23. MacArthur, R. H. & Wilson, E. O. *The Theory of Island Biogeography* (Princeton Univ. Press, 1967).
24. Siegel, D., Kinlan, B., Gaylord, B. & Gaines, S. Lagrangian descriptions of marine larval dispersion. *Mar. Ecol. Prog. Ser.* **260,** 83–96 (2003).
25. Hobbs, J.-P. A., Jones, G. P., Munday, P. L., Connolly, S. R. & Srinivasan, M. Biogeography and the structure of coral reef fish communities on isolated islands. *J. Biogeogr.* **39,** 130–139 (2012).
26. Shanks, A. L. Pelagic larval duration and dispersal distance revisited. *Biol. Bull.* **216,** 373–385 (2009).
27. Cowen, R. K., Lwiza, K. M. M., Sponaugle, S., Paris, C. B. & Olson, D. B. Connectivity of marine populations: open or closed? *Science* **287,** 857–859 (2000).
28. Luiz, O. J. *et al.* Adult and larval traits as determinants of geographic range size among tropical reef fishes. *Proc. Natl Acad. Sci. USA* **110,** 16498–16502 (2013).
29. Hixon, M. A. in *The Ecology of Fishes on Coral Reefs* (ed. Sale, P. F.) (Academic Press, 1991).
30. Ryberg, W. A. & Chase, J. M. Predator-dependent species-area relationships. *Am. Nat.* **170,** 636–642 (2007).
31. Stier, A. C., Hanson, K. M., Holbrook, S. J., Schmitt, R. J. & Brooks, A. J. Predation and landscape characteristics independently affect reef fish community organization. *Ecology* **95,** 1294–1307 (2014).
32. Stier, A. C., Geange, S. W., Hanson, K. M. & Bolker, B. M. Predator density and timing of arrival affect reef fish community assembly. *Ecology* **94,** 1057–1068 (2013).
33. Paulay, G. & Meyer, C. Dispersal and divergence across the greatest ocean region: do larvae matter? *Integr. Comp. Biol.* **46,** 269–281 (2006).
34. Kool, J. T., Paris, C. B., Barber, P. H. & Cowen, R. K. Connectivity and the development of population genetic structure in Indo-West Pacific coral reef communities. *Glob. Ecol. Biogeogr.* **20,** 695–706 (2011).
35. Pauly, D., Christensen, V., Dalsgaard, J., Froese, R. & Torres, F. J. Fishing down marine food webs. *Science* **279,** 860–863 (1998).
36. Branch, T. A. *et al.* The trophic fingerprint of marine fisheries. *Nature* **468,** 431–435 (2010).
37. Tolimieri, N., Samhouri, J. F., Simon, V., Feist, B. E. & Levin, P. S. Linking the trophic fingerprint of groundfishes to ecosystem structure and function in the California Current. *Ecosystems* **16,** 1216–1229 (2013).
38. Hein, A. M. & Gillooly, J. F. Predators, prey, and transient states in the assembly of spatially structured communities. *Ecology* **92,** 549–555 (2011).
39. Fahimipour, A. K. & Hein, A. M. The dynamics of assembling food webs. *Ecol. Lett.* **17,** 606–613 (2014).
40. Bode, M., Bode, L. & Armsworth, P. R. Different dispersal abilities allow reef fish to coexist. *Proc. Natl Acad. Sci. USA* **108,** 16317–16321 (2011).
41. Schleuning, M., Böhning-Gaese, K., Dehling, D. M. & Burns, K. C. At a loss for birds: insularity increases asymmetry in seed-dispersal networks. *Glob. Ecol. Biogeogr.* **23,** 385–394 (2014).
42. Salomon, Y., Connolly, S. R. & Bode, L. Effects of asymmetric dispersal on the coexistence of competing species. *Ecol. Lett.* **13,** 432–441 (2010).
43. Martinson, H. M., Fagan, W. F. & Denno, R. F. Critical patch sizes for food-web modules. *Ecology* **93,** 1779–1786 (2012).
44. Pandolfi, J. M. *et al.* Global trajectories of the long-term decline of coral reef ecosystems. *Science* **301,** 955–958 (2003).
45. Estes, J. A. *et al.* Trophic downgrading of planet Earth. *Science* **333,** 301–306 (2011).
46. Kulbicki, M. *et al.* Global biogeography of reef fishes: a hierarchical quantitative delineation of regions. *PLoS ONE* **8,** e81847 (2013).
47. Gill, A. The dynamics of prey choice in fish: the importance of prey size and satiation. *J. Fish Biol.* **63,** 105–116 (2003).
48. Pinheiro, J., Bates, D., DebRoy, S. & Sarkar, D. Linear and nonlinear mixed effects models. *R Package Version*. 3.1-117, 57 (2014).
49. R Development Core Team. *R: a Language and Environment for Statistical Computing*. R 3.0 edn (R Foundation for Statistical Computing, 2013).

Acknowledgements

The paper benefitted from discussion with C. Osenberg, M. McCoy, B. Bolker, M. O'Connor, K. Lafferty, S. McKinley, J. Samhouri, O. Shelton, R. Fletcher, T. Palmer and R. Holt and from R. Becheler's contribution to the PLD database. This work was supported by the Ocean Bridges program funded by the French American Cultural Exchange, GASPAR and RESICOD programs from Fondation pour la Recherche en Biodiversité, the National Science Foundation (Grant No. DGE-0802270 to A.M.H. and Grant No. 0801544 in the Quantitative Spatial Ecology, Evolution and Environment Program at the University of Florida), a Killam Postdoctoral Fellowship to A.C.S. at University of British Columbia and the support of the Gordon and Betty Moore Foundation to the Ocean Tipping Points project.

Author contributions

A.C.S., A.M.H. and M.K. designed the study and wrote the manuscript. V.P. gathered geospatial data. A.M.H. performed statistical and mathematical analyses and V.P. and M.K. contributed the database of fish biodiversity and larval durations in the South Pacific.

Additional information

Supplementary Information accompanies this paper at http://www.nature.com/naturecommunications

Competing financial interests: The authors declare no competing financial interests.

Reprints and permission information is available online at http://npg.nature.com/reprintsandpermissions/

How to cite this article: Stier, A. C. *et al.* Larval dispersal drives trophic structure across Pacific coral reefs. *Nat. Commun.* 5:5575 doi: 10.1038/ncomms6575 (2014).

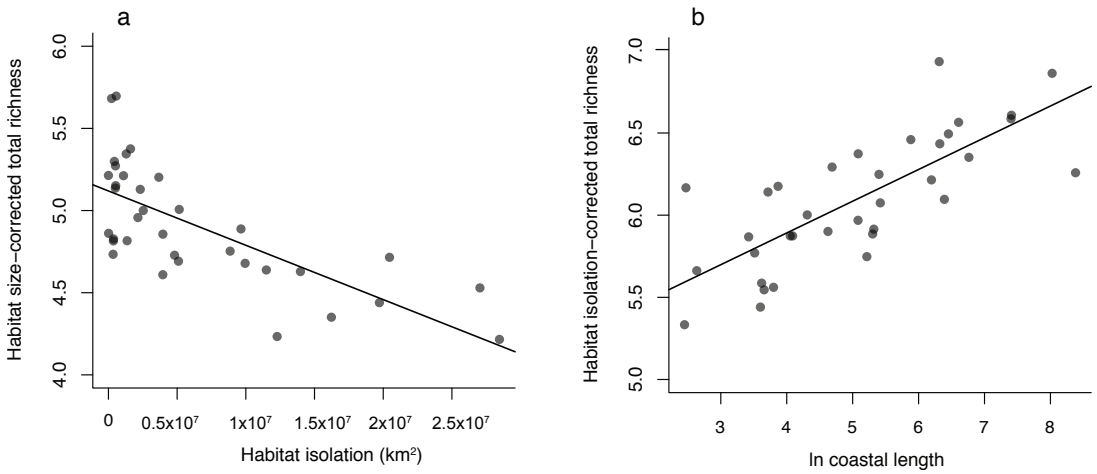

Supplementary Figure 1: Total reef fish species richness (predator richness + prey richness) as a function of predictors. (a) Habitat size-corrected total reef fish species richness as a function of habitat isolation (km^2). Total richness is corrected for habitat size based on fitted habitat size dependence: habitat size-corrected total richness = ln(total richness) $-\alpha_3 \times$ ln(coastal length), where α_3 is the fitted coefficient of ln(coastal length). Line is linear model fit to data (see Supplementary Methods section 1). (b) Habitat isolation-corrected total reef fish species richness as a function of ln coastal length (coastal length measured in km). Total richness is corrected for habitat isolation based on fitted isolation dependence: habitat isolation-corrected total richness = ln(total richness) $-\alpha_2 \times$ habitat isolation, where α_2 is the fitted regression coefficient of habitat isolation. Line is linear model fit to data (see Supplementary Methods section 1). Correcting total species richness for size or isolation allows us to plot data on bivariate plots to look only at the effect of habitat isolation or ln coastal length, respectively.

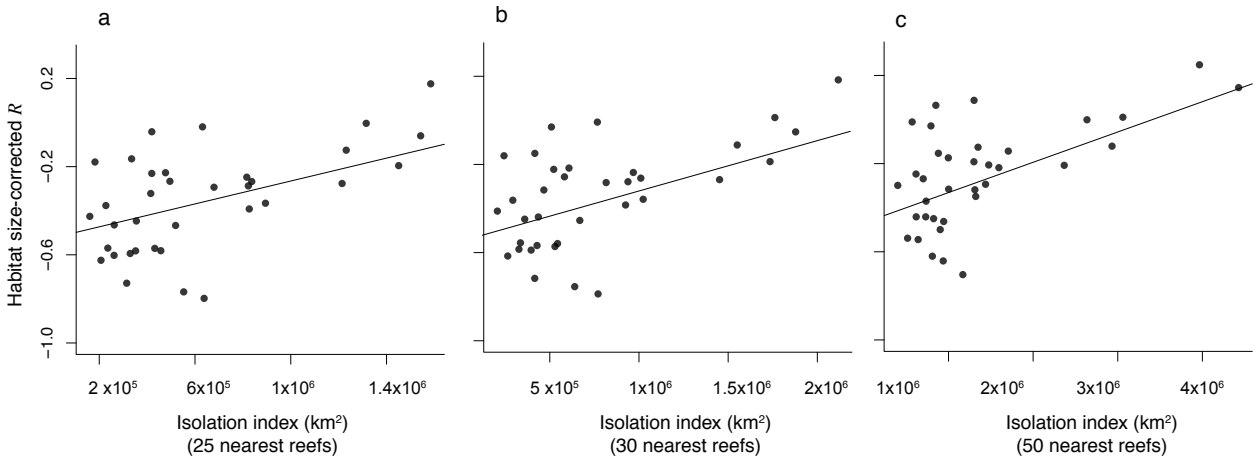

Supplementary Figure 2: Predator-prey ratio as a function of isolation index for the 35 Pacific habitats in the dataset. Lines are linear model fits to data (see Supplementary Methods section 4.1). Isolation index is measured for each focal habitat as the squared mean distance from the centroid of that focal habitat to the nearest 25 (a), 30 (b), or 50 (c) habitats that support reef-associated fishes. In each panel, predator-prey ratio is corrected for the fitted habitat size effect according to the equation: Habitat size-corrected $R = \ln(R) - \alpha_3 \times \ln(\text{coastal length})$, where α_3 is the fitted coefficient of ln(coastal length), where coastal length measured in units of km. This correction allows us to plot data on bivariate plots to look only at the effect of isolation index.

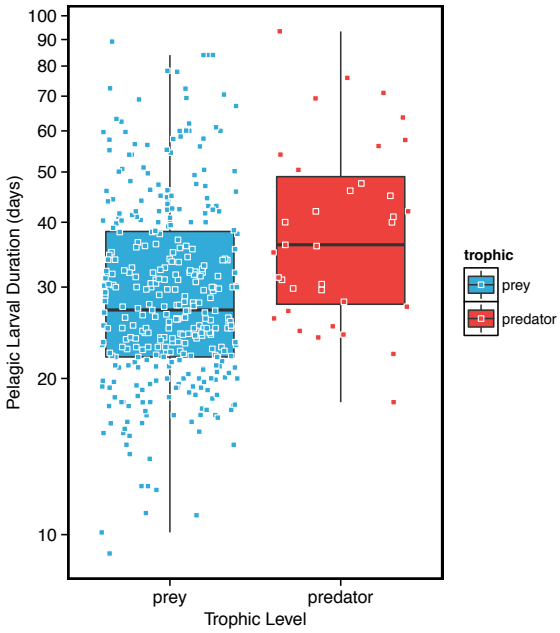

Supplementary Figure 3: Box plots depicting pelagic larval duration (PLD) data for Pacific reef fishes. Points are individual predator (red) and prey (blue) PLD values and are jittered along the x-axis for display purposes only. Black horizontal bar represents median of each trophic group. Upper and lower bounds of colored boxes represent 75th and 25th percentiles, respectively. Vertical lines extend to 95th (upper line) and 5th (lower line) percentiles.

Supplementary Table 1. Comparison among models of predator-prey ratio with and without indices of fishing pressure. Fitted models include effects of habitat isolation, coastal length, and two alternative metrics of fishing pressure for each site: human population density within 20km of the coast, and market distance (km), measured as the distance to the nearest provincial capital (see Supplementary Methods section 5). The "Iso." column gives coefficient estimates for the effect of habitat isolation. The "Fishing" column gives coefficient estimates for the fishing proxy used in the model (i.e. either market distance or log(1+ human density)). "p Iso." and "p Fishing" columns report p-values for model coefficients. The form of the fitted functions are described in Supplementary Methods section 5. All models that include habitat isolation as a predictor are within 2 AIC units of one another. Models that do not contain habitat isolation provide a much poorer fit to data.

Covariates	**Iso.**	**Fishing**	***p* Iso.**	***p* Fishing**	**AIC**	**ΔAIC**
iso., coastal length, market dist.	1.4×10^{-1}	7.6×10^{-2}	8.0×10^{-4}	7.9×10^{-2}	-4.0	0
iso., coastal length, pop. dens.	1.7×10^{-1}	-6.7×10^{-2}	2.0×10^{-4}	4.7×10^{-2}	-2.8	1.2
iso., coastal length	1.6×10^{-1}	-	2.0×10^{-4}	-	-2.5	1.5
coastal length, market dist.	-	4.9×10^{-2}	-	0.24	2.7	6.7
coastal length, pop. dens.	-	-2.0×10^{-2}	-	0.60	3.6	7.6

Supplementary Methods

1 Relationship between total richness and habitat isolation

To explore the effect of habitat isolation on total richness (predator richness + prey richness) we fitted ln(total richness) as a linear function of habitat isolation (squared distance to the nearest landmass with area greater than 10^4 km^2) and ln(coastal length) as we did for the model of predator-prey ratio described in the Main Text. We fitted spherical, exponential, rational quadratic, and Gaussian spatial autocorrelation functions. Here we report statistics from the model with the spatial autocorrelation function that yielded the lowest AIC. As has been reported in past analyses, total richness summed across trophic groups (predators + prey) decreased with increasing habitat isolation ($r^2 = 0.89$, spherical spatial autocorrelation, isolation effect: $p = 2.5 \times 10^{-5}$; coastal length effect: $p = 5.3 \times 10^{-8}$). This trend is illustrated in Supplementary Figure 1a. Supplementary Figure 1b shows the dependence of total richness on coastal length.

2 Dependence of predator-prey ratio on colonization and extinction rates

The framework developed below is based on the Equilibrium Theory of Island Biogeography developed in (3). We apply this framework to study colonization, extinction, and equilibrium species richness of species in two trophic levels (i.e. predators and prey). Thus, we depart from the assumption of (3) – that all species are equivalent in all demographic parameters – and assume instead that species within a particular trophic level are identical, but that predators and prey may differ in ways that affect their rates of colonization and extinction. When colonization and extinction of predators and prey has reached equilibrium, define the predator-prey ratio R in a local habitat as the expected number of predator species present in the community divided by the expected number of prey species present:

$$R = \frac{\mathbb{E}[S_{\text{pred}}]}{\mathbb{E}[S_{\text{prey}}]} = \frac{p^*_{\text{pred}}}{p^*_{\text{prey}}} R_{\text{pool}}, \tag{S1}$$

where S_{pred} and S_{prey} are the number of predator and prey species in a typical community, R_{pool} is the ratio of predators to prey in the regional species pool, and p^*_{pred} and p^*_{prey} are the equilibrium occurrence probabilities of total predator and prey species. Alternatively, R, could be defined as the expected value, $\mathbb{E}[S_{\text{pred}}/S_{\text{prey}}]$, rather than the ratio $E[S_{\text{pred}}]/E[S_{\text{prey}}]$. However, this formulation is similar to Equation (S1) under the conditions we wish to study. To see this, employ a 2nd order Taylor expansion of the ratio $S_{\text{pred}}/S_{\text{prey}}$, and assume S_{pred} and

S_{prey} are distributed independently and according to binomial distributions with parameters (n_2, p_2^*) and (n_1, p_1^*), respectively. Then $\mathbb{E}\left[\frac{S_{\text{pred}}}{S_{\text{prey}}}\right] \approx \frac{n_2 p_2^*}{n_1 p_1^*} + O\left[\frac{n_1 p_1^*}{(n_2 p_2^*)^2}\right]$. In the scenario considered in the Main Text, the species pool is very large (i.e. $n_i >> 1$) and, although p_i may become small, we do not expect the product $n_i p_i^*$ to be small; the numbers of predator and prey species are at least of order 100, even in the most species poor communities in our dataset. Thus, $R \approx n_2 p_2^*/(n_1 p_1^*) = \mathbb{E}[S_{\text{pred}}]/\mathbb{E}[S_{\text{prey}}] = (p_2^*/p_1^*) R_{\text{pool}}$ provides a reasonable approximation of $\mathbb{E}[S_{\text{pred}}/S_{\text{prey}}]$ in the regime of interest.

Equation (S1) relies on the assumption that species within a trophic level colonize independently of one another and are all equally likely to be present in a given habitat. The number of species in trophic level i occurring in a particular habitat is a binomial random variable, with mean $n_i p_i^*$, where n_i is the total richness of trophic level i in the regional species pool, and p_i^* is given by

$$p_i^* = \frac{1}{1 + E_i/C_i}. \tag{S2}$$

Here C_i is the colonization rate of species in the ith trophic level (i.e., predators or prey), and E_i is the extinction rate of species in the ith trophic level. Solving for predator and prey equilibria independently assumes that the dynamics of predators and prey are decoupled from one another. We show in Section 4.2 below that the basic intuition developed under this assumption can hold even if predators and prey are coupled by trophic dependencies. Combining equations (S1) and (S2) shows that

$$R = \frac{C_{\text{pred}} E_{\text{prey}}}{C_{\text{prey}} E_{\text{pred}}} \left[\frac{C_{\text{prey}}/E_{\text{prey}} + 1}{C_{\text{pred}}/E_{\text{pred}} + 1}\right] R_{\text{pool}}. \tag{S3}$$

Equation (S3) can be simplified in many cases. For instance, in many local communities, the probability of any given species being present will be small (i.e. $p_i^* << 1$). It follows from equation (S2) that $C_i/E_i = \frac{p_i^*}{1-p_i^*}$ will also be small, yielding the approximate proportionality

$$R \propto \left(\frac{C_{\text{pred}}}{C_{\text{prey}}}\right)\left(\frac{E_{\text{prey}}}{E_{\text{pred}}}\right). \tag{S4}$$

Equation (S4) shows that predator-prey ratio increases as the ratio of predator colonization rate to prey colonization rate increases, and increases as the ratio of prey extinction rate to predator extinction rate increases.

3 Linking predator-prey ratio to habitat isolation through larval dispersal

In the Main Text, we show that predatory reef fish species have longer pelagic larval durations (PLDs), on average, than prey. Here we use a diffusion-advection-mortality model of larval dispersal (4) to show how such a difference in PLD of predators and prey can induce a positive correlation between predator-prey ratio and habitat isolation. We assume larvae are produced annually and released from a large source population at a single geographic location. Once in the plankton, directional ocean currents cause advection of larvae and local turbulence and other flow features causes larvae to spread. At some time τ_i, all individuals in trophic level i settle out of the water column and arrive as immigrants on any reef present at their location. In two dimensions, the colonization rate of species in trophic group i, at location (x, y) is proportional to the concentration of larvae at (x, y), I_i:

$$C_i \propto I_i = \frac{N_i}{4\pi\sigma\tau_i} e^{-\mu_i\tau_i} \exp\left[\frac{-(x - x_0 - u\tau_i)^2}{4\sigma\tau_i}\right] \exp\left[\frac{-(y - y_0 - v\tau_i)^2}{4\sigma\tau_i}\right], \tag{S5}$$

where x_0 and y_0 are the x- and y-coordinates of the source where larvae are released, u and v are current velocities in the x and y directions respectively, N_i is the number of larvae released, σ is the effective diffusivity of larvae (assumed to be equal for predators and prey), τ_i is PLD, and μ_i is mortality rate. To see the effect of differences in PLD between predators and prey, we assume $\tau_{\text{pred}} \neq \tau_{\text{prey}}$. Defining the point of larval release as $(0, 0)$ and taking the ratio of $C_{\text{pred}}/C_{\text{prey}}$ shows, after some algebraic simplification,

$$\frac{C_{\text{pred}}}{C_{\text{prey}}} \propto \frac{N_{\text{pred}}\tau_{\text{prey}}}{N_{\text{prey}}\tau_{\text{pred}}} \exp\left[-(\tau_{\text{pred}} - \tau_{\text{prey}})(\mu + \frac{u^2 + v^2}{4\sigma})\right] \exp\left[\frac{(\tau_{\text{pred}} - \tau_{\text{prey}})d^2}{4\sigma\tau_{\text{pred}}\tau_{\text{prey}}}\right], \tag{S6}$$

where d is the distance between the source of larvae and the focal habitat, and we assume that habitat area is small enough so that the number of larvae in trophic group i available to colonize a habitat of area A centered at (x, y) can be approximated as $I_i(x, y) \times A$.

In Equation (S4), E_i will not generally depend directly on d. Thus, the effect of habitat isolation on Equation (S4) is determined by the effect of isolation on the ratio $C_{\text{pred}}/C_{\text{prey}}$. Substituting Equation (S6) into Equation (S4) shows that the sign of $(\tau_{\text{pred}} - \tau_{\text{prey}})$ determines whether R increases or decreases with increasing habitat isolation. When predatory species have longer PLDs than prey species (i.e. $\tau_{\text{pred}} > \tau_{\text{prey}}$), the ratio of the arrival rate of predator species to the arrival rate of prey species (i.e. $C_{\text{pred}}/C_{\text{prey}}$) will be greater in more isolated habitats than in more proximate habitats. Thus, under the assumptions described above, differences in PLD are sufficient to generate the qualitative pattern of increasing predator-prey ratio with increasing habitat isolation observed in our data.

An interesting feature of Equation (S6) is that the ratio of predator to prey colonization rates changes symmetrically (i.e. isotropically) about the point of larval release, regardless of the magnitude and direction of advective currents. For example, suppose a particular habitat acts as a source for islands down and up current. Although Equation (S5) predicts that the raw numbers of predator and prey larvae arriving at down and up current islands will differ, the predator prey ratio on the islands should be the same if the distances between the islands and the source are the same. This symmetry is broken when multiple sources contribute larvae to a focal habitat (see below).

4 Sensitivity to model assumptions

4.1 Multiple sources and alternative metrics of habitat isolation

To consider larval input from many source populations, it is necessary to reformulate Equation (S6). In general, predator-prey ratio need not be isotropic about sources when multiple sources are present. The arrival rate of immigrants and, therefore, $C_{\text{pred}}/C_{\text{prey}}$ will depend on the locations of sources and the directions and magnitudes of advecting currents. However, in the special case in which dispersal from all sources is symmetric, it is possible to make a general statement about the conditions under which more isolated habitats will have higher predator-prey ratios.

Here we derive a rigorous metric of habitat isolation, the *isolation index*, that can be applied when larvae arrive at a focal island from multiple sources. We will show that if $\tau_{\text{pred}} > \tau_{\text{prey}}$, predator-prey ratio will increase with increasing isolation. However, here "isolation" is computed using the distances to multiple sources, rather than the distance to a single dominant source of larvae.

Consider a scenario in which predator and prey immigrants arrive from many source populations. Assume that predator and prey larvae are produced at the same locations and the concentration of larvae dispersing from each source decays isotropically about the source. For a particular trophic level, Equation (S5) is given by

$$C_{i,j} = \gamma \frac{N_{i,j}}{4\pi\sigma\tau_i} e^{-\mu_i \tau_i} \exp\left[\frac{-d_j^2}{4\sigma\tau_i}\right] = \kappa_{i,j} e^{-\beta_i d_j^2}, \tag{S7}$$

where the subscript j denotes the jth source that supplies larvae to the focal island, γ is a positive constant that relates larval concentration to colonization rate, $\kappa_{i,j} = \gamma \frac{N_{i,j}}{4\pi\sigma\tau_i} e^{-\mu_i \tau_i}$, and $\beta_i = (4\sigma\tau_i)^{-1}$. Total colonization rate at a focal habitat is proportional to the sum of colonization rates from all sources that supply larvae to that habitat,

$$C_i = \kappa_{i,1} e^{-\beta_i d_1^2} + \kappa_{i,2} e^{-\beta_i d_2^2} + ... + \kappa_{i,n} e^{-\beta_i d_n^2}. \tag{S8}$$

Let $\overline{d}$ denote the mean distance from the focal habitat to the nearest h sources, and $\hat{d} := d/\overline{d}$. Each term on the right hand side of Equation (S8) can be rewritten, $\kappa_{i,j}e^{-\beta_i\overline{d}^2\hat{d}^2}$. For simplicity, assume that $\kappa_{i,j}$is the same for all islands, but may differ between predators and prey (i.e. $\kappa_{i,j} = \kappa_i$). Assume that the number of sources serving a particular island is large, such that it is sensible to write

$$C_i = \kappa_i \int_0^\infty e^{-\beta_i \overline{d}\hat{d}^2} f(\hat{d}^2) d\hat{d}^2, \tag{S9}$$

where $f(\hat{d}^2)$ is a probability density describing the distribution of squared normalized distances between the focal island and its sources. We can make the relatively unrestrictive assumption that $f(\hat{d}^2)$ has a gamma density

$$f(\hat{d}^2) = \frac{(\hat{d}^2/b)^{c-1}e^{-\hat{d}^2/b}}{b\Gamma(c)}, \tag{S10}$$

where $b,\ c > 0$ are parameters, Γ is the gamma function, and the expected value of $f(\hat{d}^2) = bc$ (5). Under this assumption, the colonization rate of the ith trophic level at a focal island with mean distance to the nearest h islands, $\overline{d}$, has the form

$$C_i = (b\beta_i\overline{d}^2 + 1)^{-c}. \tag{S11}$$

This approach is valid for multiple islands differing in isolation if more isolated islands are simply farther from all sources by a constant factor (i.e., if the distances between any given focal island and its sources are l_1, l_2, l_3..., the distances between any other island and its sources can be written $r_1 = al_1$, $r_2 = al_2$, $r_3 = al_3$..., for some positive constant a). The form of Equation (S11) is familiar in economics as it is related to the notion of non-exponential discounting arising from uncertain hazard rates (6). Equation (S11) can be found using the method of Laplace transforms, applied to the gamma distributed random variable $\hat{d}^2$. Substituting Equation (S11) into Equation (S4) gives

$$R \propto \frac{C_{\text{pred}}}{C_{\text{prey}}} \propto \left[\frac{b\beta_{\text{prey}}\overline{d}^2 + 1}{b\lambda\beta_{\text{prey}}\overline{d}^2 + 1}\right]^c, \tag{S12}$$

where $\lambda = \tau_{\text{prey}}/\tau_{\text{pred}}$ as in the Main Text. Equation (S12) shows that the condition $\tau_{\text{pred}} > \tau_{\text{prey}}$ is sufficient to ensure that predator-prey ratio increases with increasing isolation index $\overline{d}^2$.

Supplementary Figure 2 shows ln(predator-prey ratio) as a function of isolation index using squared mean distance to the nearest 25 ($h = 25$, a), 30 ($h = 30$, b) and 50 ($h = 50$, c) potential sources as a measure of isolation index $\overline{d}^2$.

To compute these mean distances, we used a Behrmann projection to divided the world into cells (200 × 200 km at the equator) from which we retained only cells containing reef fish habitat (i.e. coast or coral reef). These cells represent potential sources and for each location we computed the mean distance from the location to the h nearest sources using great circle distance (1). Rather than fitting the nonlinear (S12) directly to data, we observed (by Taylor expansion) that the logarithm of (S12) can be well approximated by a linear function of $\overline{d}^2$ when $b\beta_{\text{prey}}\overline{d}^2$ and $b\lambda\beta_{\text{prey}}\overline{d}^2$ are between zero and one. This approximation allows us to rely on more robust linear (vs. nonlinear) fitting techniques, allowing us to incorporate heterogeneous variance and spatial autocorrelation. It provides a good fit to the predator-prey ratio data (Supplementary Figure 2). We used generalized least-squares to fit a model of the form: $\ln(R) = \alpha_1 + \alpha_2 \times \text{isolation index} + \alpha_3 \times \ln(\text{coastal length}) + \Omega$, where α_j are regression coefficients and Ω is an error term that incorporates spatial autocorrelation and normally distributed errors with heterogeneous variance (through an exponential variance model) to account for the apparent decreasing variance with increasing mean evident in Supplementary Figure 2. Predator-prey ratio increased strongly with increasing isolation index (effect of isolation index, nearest 25 sources: $p = 4.4 \times 10^{-6}$; 30 sources: $p = 1.9 \times 10^{-2}$; 50 sources: $p = 3.3 \times 10^{-4}$). The increasing predator-prey ratio with increasing isolation index is consistent with the findings presented in the Main Text: that predator-prey ratio increases with increasing habitat isolation.

4.2 Dependence of predators on their prey

To determine whether the results presented above hold when the colonization and persistence of a species depends on the presence of its prey, we expand on the trophic island biogeography framework of Gravel *et al.* (7). When predators are coupled to their prey, a predator species will fail to colonize a habitat if all of its prey species are absent and will go extinct when its last prey species goes extinct. This can be accounted for by modifying the equation describing the dynamics of $p_{i,j}$:

$$\frac{dp_{i,j}}{dt} = C_{i,j}q_{i,j}(1 - p_{i,j}) - (E_{i,j} + \omega_{i,j})p_{i,j}, \tag{S13}$$

where the intrinsic colonization rate $C_{i,j}$ is assumed to be a function of habitat isolation and $E_{i,j}$ is intrinsic extinction rate in a given habitat, $q_{i,j}$ represents the probability that the prey of species j in trophic level i is present given that the speces j in level i is absent, and $\omega_{i,j}$ is the rate at which species j in trophic level i goes extinct because of the loss of its last prey species (7). Intrinsic extinction rate is the rate of extinctions that are not directly due to the loss of prey species (e.g., extinction due to natural disaster). Equation (S13) has equilibrium $p^*_{i,j} = \frac{1}{1+\frac{E_{i,j}+\omega_{i,j}}{C_{i,j}q_{i,j}}}$. We have added the species index j for clarity and will later show that it disappears when we assume that all species within a particular trophic level are equivalent in all life history parameters.

The primary result of (7) is to derive the parameters q and ω as expected values of random variables in a stochastic coloniztion-extinction process. The authors then assume that colonization-extinction dynamics of species in a particular dietary class (i.e., species that have the same resource breadth) can be studied using a deterministic ordinary differential equation with parameters q, ω, E and C, analogous to Equation (S13). We adapt this framework to model the reef fish component of coral reef food webs. Though we apply this approach to reef fish, our results are generic and could be applied to a sub-component of any food web, so long as the assumptions discussed below are satisfied.

From this point through Equation (S17) our derivation parallels that of (7) with the only major modification being that we track the trophic level that each species belongs to. Denote the presence of species j in trophic level i, $X_{i\,j}$. Furthermore, define $Y_{i\,j}$ as an indicator variable that is equal to 1 when at least one of the prey of j is present given that species j is absent, and 0 otherwise. We wish to derive $q_{i\,j}$, the expectation that species j has at least one prey species present, given that it is absent:

$$q_{i,j} = 1 - \mathbb{E}\left[\prod_{k \in G_{i,j}} (1 - X_{i-1,k}) | X_{i,j} = 0\right], \tag{S14}$$

where $G_{i,j}$ denotes the set of prey species, any of which is sufficient to sustain species j in trophic level i, and the number of such species $|G_{i,j}|$ is denoted $g_{i,j}$. In keeping with the assumption that species within a trophic level are equivalent, we assume that all species in trophic level i rely on the same number of species in trophic level $i-1$ (i.e. $g_{i,j} = g_{i,k}\ \forall\ j,\ k$). Following (7), we assume that the conditional expectation in Equation (S14) is equal to the marginal expectation $\mathbb{E}[\prod_{k \in G_{i,j}}(1 - X_{i-1,k})]$. Moreover, since all species in trophic level $i-1$ are also assumed to be identical, $\mathbb{E}[X_{i-1}] = \mathbb{E}[X_{i-1,j}] = \mathbb{E}[X_{i-1,k}]\ \forall\ j,\ k$, and

$$q_{i,j} = q_i \approx 1 - \prod_{k \in G_{i,j}} (1 - \mathbb{E}[X_{i-1,k}]) = 1 - (1 - \mathbb{E}[X_{i-1}])^{g_i} = 1 - (1 - p^*_{i-1})^{g_i}, \tag{S15}$$

where p^*_{i-1} denotes the equilibrium occurrence probability of species in the $i-1$th trophic level. The assumption that all species in trophic level i rely on the same number of prey species g_i, eliminates the need to index species j. To derive a similar expression for $\omega_{i\,j}$, note that $\omega_{i\,j}$ is the rate at which the last prey of species j goes extinct from a local habitat. This is just the probability that a particular prey species is the last prey of species j, times the extinction rate of that prey species, summed over all prey of species j:

$$\omega_{i,j} = \mathbb{E}\left[\sum_{k \in G_{i\,j}} E_{i-1,k} X_{i-1,k} \left(\prod_{z \in G_{i,j};\, z \neq k} (1 - X_{i-1,z}) | X_{i,j} = 0\right)\right]. \tag{S16}$$

Under the assumptions described above, this reduces to

$$\omega_{i,j} = \omega_i \approx g_i E_{i-1} p^*_{i-1} (1 - p^*_{i-1})^{g_i}. \tag{S17}$$

The species subscript j has again been dropped because all species within a particular trophic level are assumed to be equivalent. Solving for Equation (S13) for equilibrium, substituting Equations (S15) and (S17) for q_i and ω_i, and simplifying leads to the expression for the equilibrium occupancy of species in the ith trophic level, where $i > 0$:

$$p^*_i = \frac{\frac{C_i}{E}\left[1 - (1 - p^*_{i-1})^{g_i}\right]}{1 + \frac{C_i}{E}\left[1 - (1 - p^*_{i-1})^{g_i} + g_i (1 - p^*_{i-1})^{g_i} q_{i-1}\right]}, \tag{S18}$$

where intrinsic extinction rates E are assumed to be equal for species in different trophic levels. The ratio of species in two adjacent trophic levels can be modeled by substituting (S18) into Equation (S1). Indexing for predator (2) and prey (1) reef fish leads to the expression for the equilibrium occurrence probability of predatory reef fish:

$$p^*_2 = \frac{\frac{C_2}{E}\left[1 - (1 - p^*_1)^{g_2}\right]}{1 + \frac{C_2}{E}\left[1 - (1 - p^*_1)^{g_2} + g_2 (1 - p^*_1)^{g_2} q_1\right]}, \tag{S19}$$

where $q_1 = 1$. We assume that prey occurrence probability is described by $p^*_1 = \frac{1}{1 + \frac{E}{C_1}}$. Assuming $q_1 = 1$ implies that prey species are not typically prohibited from colonizing or driven extinct by the absence of their resources. In other words, we assume that when a prey species arrives in a habitat, it has the resources it needs to survive there, and those resources do not disappear. Dividing Equation (S19) by p^*_1 yields an expression for predator-prey ratio, R, that incorporates a trophic dependence of predators on prey.

For short to intermediate distances $R = p^*_2 / p^*_1$ can be approximated by the relation

$$R \approx H_1 + H_2 \frac{C_{\text{pred}}}{C_{\text{prey}}}, \tag{S20}$$

where H_1 and H_2 are positive constants. This is the same proportionality between R and $\frac{C_{\text{pred}}}{C_{\text{prey}}}$ derived in the Main Text, except that there is a constant offset of H_1. The conclusion that predator-prey ratio will increase as the ratio of $C_{\text{pred}}/C_{\text{prey}}$ increases is unchanged. We reach the approximation described by Equation (S20) by noting that $(1 - p^*_1)^{g_2}$ in Equation (S19) is approximately equal to zero when p^*_1 is not too small or g_2 is large. Biologically, this means that the probability of any given prey species being present at the focal site is not too small, or each predator species is capable of feeding on many different prey species. This is intuitive: if predators are generalists or prey are species-rich enough that many suitable prey are likely to be present for each predator, small changes in

prey richness have little direct effect on predator richness and we find a similar expression for R to that derived in the Main Text. Equation (S20) yields the same qualitative conclusions reached in the Main Text–that R increases from some initial value in proportion to the ratio of predator to prey colonization rates. However, we emphasize that Equation (S18) provides a rigorous means of reaching this conclusion and allows us to predict the functional form of the relationship between R and C_2/C_1 in addition to yielding qualitative conclusions about scaling.

Equation (3) in the Main Text shows that R increases indefinitely with increasing isolation distance, so long as predator PLD exceeds prey PLD. When the dependence of predators on prey is incorporated, this is not the case. For very large distances, p_1^* and p_2^* are small and Equation (S20) is not valid. Instead, R can be approximated by the expression

$$R \approx \frac{C_{\text{pred}}}{E/g_2 + C_{\text{pred}}}, \tag{S21}$$

which goes to zero as C_{pred} goes to zero for very large distances. This approximation results by assuming p_1^* is very small (because C_1 is assumed to be very small) and observing that $(1 - p_1^*)^{g_2} \approx 1 - g_2 p_1$ for very small p_1^*, and that terms of order $C_1 C_2/E^2$ vanish. Equation (S21) shows that predator-prey ratio does not increase indefinitely as isolation distance increases and colonization rates approach zero. This is because predators rely on prey, and go extinct from communities very rapidly as prey richness goes to zero. This result is reassuring because predators should not be able to persist as the number of prey species becomes very small.

Adding trophic coupling between predators and prey retains the essential behavior predicted in the Main Text for short to intermediate isolation distances. Additionally, it predicts that predator-prey ratio will decline after some critical distance is exceeded because, although predator larvae may continue to arrive at an island, too few prey species are present to support them. The data shown in the Main Text do not indicate a major decline in predator-prey ratio for large distances, perhaps suggesting that prey availability is not a major constraint limiting predator richness in the habitats included in our analysis.

4.3 Dynamics when predators consume juveniles of all species

In the previous section, we assumed that each predator species can consume a subset of the species in the prey trophic level. Some piscivorous reef fish prey on a wide variety of juvenile fish, regardless of the future trophic status of those fish (i.e., adult piscivores consume juvenile piscivores in addition to other species). Fully considering intra-guild predation and cannibalism would require a more detailed model. However, we can use the model developed above to explore extreme cases. For example, suppose each predator can persist by consuming individuals of any predator species (including its own species), or by consuming prey. Then the $q_{i,j}$ term in Equation (S13) will be large

(i.e., close to one) for predators because any colonizing predator can persist by consuming juveniles of any species that is already present. The $\omega_{i,j}$ term in Equation (S13) is equal to zero because, again, a predator can always avoid extinction by consuming juvenile conspecifics. Setting $q_{i,j}$ to one and $\omega_{i,j}$ to zero recovers the uncoupled equation for p_i presented in the Main Text. Interestingly, this extreme trophic generalization releases predators from the constraints imposed by limited dispersal capacity of prey. This may partially explain why predator-prey ratio in the Pacific reef fish data does not decrease appreciably in highly isolated habitats as one would expect it to if each predator relied solely on a small subset of prey.

5 Relationship between predator-prey ratio and fishing pressure

To determine whether the pattern of increasing predator-prey ratio with increasing spatial isolation could be due to spatial variation in human-induced extinctions, we computed two proxies for fishing pressure: population density in coastal regions of each site and distance from each site to the nearest provincial capital. Both of these proxies have been used as indices of fishing pressure in recent analyses of the effect of fishing on pacific reef fish (see (8) and references therein). To compute human coastal population density, we compiled human population sizes for the 35 sets of islands used in our analysis. We computed coastal human population density (henceforth "human density") as the density of humans within a 20km coastal belt around each island or set of islands using the Gridded Population of the World dataset (GPW3, (9)). To estimate the distance to the nearest large market (henceforth "market distance") we followed the analysis of (8) and computed the great circle distance from the centroid of each site in our dataset to the nearest provincial capital.

In the model of predator-prey ratio derived above, both colonization and extinction rates influence predator-prey ratio (Equation S4). If fishing pressure on predatory reef fish influences predator-prey ratio, the effect ought to occur via high predator extinction rates in regions subject to high fishing pressure. Since there is no reason that effects of fishing and effects of larval dispersal on predator-prey ratio must be mutually exclusive, we fitted a series of statistical models with habitat isolation, coastal length, and a proxy of fishing pressure as predictors. In each model, we fitted $\ln(R)$ as a linear function of covariates. The covariates used were squared isolation distance (i.e. habitat isolation described in the Main Text), ln coastal length, ln(1 + human density), and market distance. ln(1 + human density) was used as a predictor instead of untransformed human density because ln transformation appeared to linearize the relationship between human density and ln predator-prey ratio. For each model shown in Supplementary Table 1, we fitted the same spatial autocorrelation models described in *Methods* in the Main Text and report results from the statistical model with the lowest AIC score from among these. To facilitate comparison of effect sizes, we scaled and centered each predictor variable prior to analysis by subtracting its mean and dividing by its standard deviation. The condition numbers of predictor matrices were low (condition number 1.9 for squared

isolation distance, ln coastal length, and ln(1 + human density); 1.8 for squared isolation distance, ln coastal length, and market distance) indicating that multicolinearity among predictor variables was minimal.

If selective overfishing of top predators were solely responsible for the patterns reported in the Main Text, we would expect that models including indices of fishing pressure, but excluding habitat isolation would provide the best compromise between parsimony and goodness of fit. Supplementary Table 1 shows that this is not the case. Models that exclude habitat isolation as a predictor have AIC scores that are substantially higher (2.7, and 3.6) than models that include the effect of habitat isolation (AIC $\leq$ -2.5), indicating that dropping habitat isolation as a predictor causes a substantial decrement in model fit. By contrast, all models that include habitat isolation as a predictor are within 2 AIC units of the model with the lowest AIC even when indices of fishing pressure are excluded. This suggesting that models with and without fishing pressure provide similar fits to the data so long as the predicted relationship between predator-prey ratio and habitat isolation is included. Taken together, these results suggest that fishing pressure alone is not sufficient to explain the observed patterns in predator-prey ratio.

6 Prey designation

Our analyses focus on the reef fish component of coral reef food webs. Our goal was to identify piscivorous top predators and the primary species they feed upon. Because marine predators are often gape limited and deterred by unpalatable species, we chose a definition of "prey" in the Main Text that we believed most accurately characterizes the reef fish species that are commonly targeted and consumed by reef fish top predators (i.e., species with a maximum reported total length less than 20cm and high palatability). We will refer to the designation of prey used in the Main Text as "moderate". To evaluate the sensitivity of our results to this definition of prey, we re-analyzed data using two alternative definitions: a more inclusive definition of prey, and a more exclusive definition of prey. As discussed below, neither of these alternative schemes for designating which species are considered prey alters the qualitative conclusions of our analyses.

To define prey more inclusively, we included all prey species, regardless of adult body size or palatability (see *Methods* of Main Text for palatability scoring). We then repeated the analyses presented in the Main Text. We will refer to this definition of prey as "inclusive". As was seen for the moderate designation of prey, when we analyzed the ln of predator and prey species richness as a function of habitat isolation (i.e., analysis depicted in Figure 2B in the Main Text) using all prey species that met the inclusive prey designation, both predator and prey ln species richness declined with increasing habitat isolation ($p = 1.6 \times 10^{-4}$) and the effect of isolation on prey was greater than the effect of isolation on predators (isolation $\times$ type interaction: 9.5×10^{-6}). The model explained a large proportion of the variance in ln predator and prey species richness ($r^2 = 0.78$). The model of ln predator-prey ratio as a function of habitat isolation and ln coastal length (analysis depicted in Figure 2C in the Main Text) also

yielded the same qualitative result when we used the inclusive designation of prey; ln predator-prey ratio increased with increasing habitat isolation ($p = 1.8 \times 10^{-4}$), and habitat isolation and ln coastal length collectively explained 44% of the variance in ln predator-prey ratio. Finally, the inclusive prey designation resulted in a similar fit of the model describing predator species richness as a function of prey diversity (i.e., model depicted in Figure 4 in the Main Text). The generalized nonlinear least squares model describing predator species richness as a power function of prey species richness indicated a power function exponent significantly different from zero ($p = 4.9 \times 10^{-16}$) with an estimate of 0.6 (95% CI [0.5, 0.68]), indicating that the exponent was also less than 1. Again, the power function provided a better description of the data than a linear function (AIC power = 313; AIC linear = 317), indicating that predator-prey ratio decreased as total diversity increased.

As an alternative to moderate and inclusive designations of prey, we used a more restrictive designation of prey that only included prey with adult size less than 10cm and a palatability score of one. The logic behind this metric was to explore the extreme in which only small, highly palatable species are considered to be prey. We note that this restrictive metric likely excludes intermediate-sized prey species that are commonly targeted by reef fish top predators, but we include it for comparison to the prey designations discussed previously. We will refer to this designation of prey as "restrictive". As was seen for the moderate and inclusive designations of prey, when we analyzed the ln of predator and prey species richness as a function of habitat isolation using the restrictive prey designation, both predator and prey ln species richness declined with increasing habitat isolation ($p = 1.9 \times 10^{-3}$). The effect of isolation on prey was greater than the effect of isolation on predators (isolation $\times$ type interaction: 4.7×10^{-5}). Again, the model explained a much of the variance in ln predator and prey species richness ($r^2 = 0.65$). The model of ln predator-prey ratio as a function of habitat isolation and ln coastal length also yielded the same qualitative result when we used the restrictive designation of prey; ln predator-prey ratio increased with increasing habitat isolation ($p = 5.1 \times 10^{-3}$, $r^2 = 0.39$). Finally, the generalized nonlinear least squares model describing predator species richness as a power function of restrictive prey species richness indicated a power function exponent significantly different from zero ($p = 3.5 \times 10^{-14}$), with an estimate of 0.51 (95% CI [0.42, 0.6]), indicating that the exponent was also less than 1. Again, the power function provided a better description of the data than a linear function (AIC power = 321; AIC linear = 322), though the differences in relative model fit were less pronounced than when we used a less restrictive prey designation. Overall, using the restrictive prey designation did not change any of the results presented in the Main Text.

7 Pelagic larval duration data

The raw predator and prey PLD data are shown in Supplementary Figure 3. These data are included as Supplementary Data to the Main Text. The analysis that compares mean predator PLD and mean prey PLD is described

in the Figure (2) caption of the Main Text.

Supplementary References

[1] Parravicini, V, and M Kulbicki, D R Bellwood, A M Friedlander, J E Arias-Gonzalez, P Chabanet, S R Floeter, R Myers, L Vigliola, S DÁgata, and D Mouillot, (2013) Global patterns and predictors of tropical reef fish species richness. *Ecography* 36:1254-1262.

[2] Pinheiro, J, D Bates, S DebRoy, D Sarkar and R Core Team (2014) nlme: Linear and Nonlinear Mixed Effects Models. R package version 3.1-115 http://CRAN.R-project.org/package.

[3] MacArthur, R, and E O Willson (1967) *The Theory of Island Biogeography* (Princeton University Press, Princeton NJ).

[4] Hill, A E (1991)Advection-diffusion-mortality solutions for investigating pelagic larval dispersal. *Marine Ecology Progress Series* 70:117-128.

[5] Evans, M, N Hastings, and J B Peacock (2000) *Statistical Distributions* (Wiley, New York NY).

[6] Sozou, P D (1998) On hyperbolic discounting and uncertain hazard rates. *Proc. R. Soc. Lond. B* 265:2015-2020.

[7] Gravel, D, F Massol, E Canard, D Moilliot, and N Moquet, N (2011) Trophic theory of island biogeography. *Ecology Letters* 70:117-128.

[8] Cinner, J, E, N A J Graham, C Huchery, and M A MacNeil (2013) Global effects of local human population density and distance to markets on the condition of coral reef fisheries *Conservation Biology* 27:453-458.

[9] Center for International Earth Science Information Network (2005) *Gridded population of the world, Version 3 (GPWv3) Data Collection.* (Columbia University, Palisades, NY).